

Magnesium Fluoride-Dependent Binding of Small G Proteins to Their GTPase-Activating Proteins[†]

Debbie L. Graham,^{‡,§} John F. Eccleston,[‡] Chun-Wa Chung,[§] and Peter N. Lowe^{*,§}

Division of Physical Biochemistry, National Institute for Medical Research, The Ridgeway, Mill Hill, London NW7 1AA, United Kingdom, and Glaxo Wellcome Medicines Research Centre, Gunnels Wood Road, Stevenage, Hertfordshire SG1 2NY, United Kingdom

Received June 14, 1999; Revised Manuscript Received September 10, 1999

ABSTRACT: GTPase-activating proteins (GAPs) enhance the intrinsic GTPase activity of small G proteins, such as Ras and Rho, by contributing a catalytic arginine to the active site. An intramolecular arginine plays a similar role in heterotrimeric G proteins. Aluminum fluoride activates the GDP form of heterotrimeric G proteins, and enhances binding of the GDP form of small G proteins to their GAPs. The resultant complexes have been interpreted as analogues of the transition state of the hydrolytic reaction. Here, equilibrium binding has been measured using scintillation proximity assays to provide quantitative information on the fluoride-mediated interaction of Ras and Rho proteins with their respective GAPs, neurofibromin (NF1) and RhoGAP. High-affinity fluoride-mediated complex formation between Rho•GDP and RhoGAP occurred in the absence of aluminum; however, under these conditions, magnesium was required. Additionally, the novel observation was made of magnesium-dependent, fluoride-mediated binding of Ras•GDP to NF1 in the absence of aluminum. Aluminum was required for complex formation when the concentration of magnesium was low. Thus, either aluminum fluoride or magnesium fluoride can mediate the high-affinity binding of Rho•GDP or Ras•GDP to GAPs. It has been reported that magnesium fluoride can activate heterotrimeric G proteins. Thus, magnesium-dependent fluoride effects might be a general phenomenon with G proteins. Moreover, these data suggest that some protein•nucleotide complexes previously reported to contain aluminum fluoride may in fact contain magnesium fluoride.

Small GTPases belonging to the Ras superfamily control a wide range of intracellular signaling events (1, 2). They cycle between an inactive GDP-bound form and an active GTP-bound form. The GTP form binds effector molecules, which transmit downstream signals. They are down-regulated by GTPase-activating proteins (GAPs),¹ which stimulate their slow intrinsic GTPase activity. Recent insights into the mechanism of GAPs obtained through mutagenesis and structural studies show that GAPs act as enzymes by contributing a catalytic arginine to the active site and stabilizing the transition state for hydrolysis of protein-bound GTP (3–11).

Heterotrimeric G proteins are potently activated by fluoride in the presence of low concentrations of aluminum, as first shown by Sternweis and Gilman (12). Initially, aluminum fluoride was thought to be tetrahedrally coordinated and bound to GDP, acting as an analogue of the γ -phosphate of GTP (13, 14). However, the X-ray structures of G_{α} •GDP•AlF₄[−] revealed that the bound AlF₄[−] was octahedrally coordinated

with the fluorines present in a planar configuration (15, 16). Several other X-ray diffraction structures of protein•nucleotide complexes containing aluminum fluoride have now been reported (4, 6, 17–20). In each of these structures, there is either a trigonal bipyramidal or an octahedral arrangement of the ligands around the aluminum, consistent with them being analogues of their transition states. Some structures, such as Ras•RasGAP (4) and Cdc42•Cdc42GAP (20), have been interpreted as containing AlF₃; however, other structures, such as Rho•RhoGAP (6) and G_{α} (15, 16), were proposed to contain AlF₄[−].

Heterotrimeric G proteins can also be activated by fluoride in the absence of aluminum. Sternweis and Gilman (12) showed that beryllium can co-activate with fluoride, and later Higashijima et al. (21) showed that high concentrations of magnesium could replace the requirement for aluminum. This latter observation was extended by Antonny et al. (22, 23), who concluded that this was due to MgF₃[−] bound to G_{α} •GDP. Recently, Vincent et al. (24) have shown qualitatively that aluminum is not required for formation of a fluoride-mediated complex between Rho•GDP and p190 RhoGAP. This aluminum-independent binding was also attributed to the formation of a complex containing magnesium fluoride.

Here, we have confirmed that, in the absence of aluminum, magnesium can support fluoride-mediated binding of Rho•GDP to RhoGAP, and have quantified these requirements. We have also found that the requirement for aluminum for the fluoride-mediated binding of Ras•GDP to its GAP, NF1,

[†] This work was supported by the Medical Research Council, United Kingdom, and by Glaxo Wellcome.

^{*} To whom correspondence should be addressed. Telephone: +44-(0)1438 763867. Fax: +44(0)1438 764818. Email: PL44712@ggr.co.uk.

[‡] National Institute for Medical Research.

[§] Glaxo Wellcome Medicines Research Centre.

¹ Abbreviations: SPA, scintillation proximity assay; DTT, dithiothreitol; GAP, GTPase-activating protein; NF1, neurofibromin; AlF₃, aluminum fluoride (exact chemical species not defined); MgF₃, magnesium fluoride (exact chemical species not defined).

can be replaced by magnesium, suggesting that this is a general phenomenon for interaction of small G proteins and GAPs. A corollary of these data is that some protein-nucleotide complexes previously reported to contain aluminum fluoride may in fact contain magnesium fluoride.

EXPERIMENTAL PROCEDURES

Proteins and Nucleotide Complexes. Rho, GST-RhoGAP (wild-type and R282A mutant) (11), H-Ras residues 1–166 (8), and GST-NF1₃₃₄ (25) were purified as previously described. [³H]GDP complexes of Rho and Ras were made by incubating [8-5'-³H]GDP (NEN Life Science Products; 26 Ci/mmol; 150 μ Ci; dried down) with protein (0.8 mM), in the presence of 20 mM EDTA for 30 min at 37 °C. Then at 4 °C, MgCl₂ was added to a final concentration of 40 mM, and unbound nucleotide was removed on a 1 mL Sephadex G-25 superfine centrifuge column (26), equilibrated in 20 mM Tris/HCl, pH 7.5, 2 mM MgCl₂, 1 mM DTT. Protein concentrations were determined as described in references 11 and 27.

Scintillation Proximity Assay (SPA). Scintillation proximity assays were set up based on methods described for the interaction of RhoGAP/Rho (11) and Ras/Raf (27) and analyzed as in reference 27. The standard assay for Rho/RhoGAP contained, in a final volume of 200 μ L, 20 mM Tris/HCl, pH 7.5, 1 mM DTT, 2 mM MgCl₂, 0.2 mg·mL⁻¹ BSA, 4.5 μ g of anti-GST antibody (Molecular Probes), 0.25 μ M Rho·[³H]GDP, 0.04 μ M GST-RhoGAP, and 1.25 mg of Protein A SPA PVT beads (Amersham catalog no. RPNQ 0019). The standard assay for Ras/NF1 contained, in a final volume of 200 μ L, 50 mM Tris/HCl, pH 7.5, 2 mM DTT, 1 mM MgCl₂, 0.2 mg·mL⁻¹ BSA, 4.5 μ g of anti-GST antibody, 0.20 μ M Ras·[³H]GDP, 0.03 μ M GST-NF1, and 1.25 mg of SPA beads. Conditions differed slightly between experiments with Ras and Rho to maintain consistency with previous publications (11, 27). Control assays were also performed in the absence of GST-fusion proteins. When required, 0.11 mM AlCl₃ (from anhydrous AlCl₃ freshly dissolved in water), 20 mM NaF, or 1 mM deferoxamine mesylate were added to the assay. In experiments where the concentrations of Rho or Ras·[³H]GDP, MgCl₂, AlCl₃, or NaF were varied, all other concentrations remained constant.

Aluminum Determination. Optical emission spectrometry was carried out on a Varian Liberty 220 ICP-OE spectrometer by S. Francis. The wavelength of emission was 396.152 nm.

NMR Measurements. ¹⁹F NMR spectra were recorded at 298 K on a Bruker DRX600 spectrometer (resonance frequency for ¹⁹F = 564.68 MHz) with a dedicated 5 mm ¹⁹F-¹H probe in the normal configuration. Typically, 1500–3000 free induction decays were acquired for each experiment using 40° pulses at intervals of 2.5 s and a spectral width of 100 ppm. The spectra were initially processed without any weighting function. The smallest line width measured, 70 Hz at full width at half-height, was then used as the exponential line broadening factor in the spectra shown. Chemical shifts were referenced to an external standard of CF₃Cl at 0 ppm. NMR samples were prepared by the addition of the appropriate quantities of concentrated stock solutions of Rho·GDP, RhoGAP, and deferoxamine into 100 μ L of a solution of 50 mM Tris/HCl, pH 7.5, 5

mM NaF, 1 mM AlCl₃, 1 mM MgCl₂, 5% D₂O in a 5 mm Shigemi tube.

RESULTS

Aluminum Is Not Required for the Formation of a High-Affinity Fluoride-Dependent Complex between either Rho·GDP and RhoGAP or Ras·GDP and NF1. Equilibrium binding measurements of Rho·GDP to the GAP domain of RhoGAP were made using scintillation proximity assays (SPAs) in which GST-RhoGAP was attached to Protein A SPA beads (via anti-GST). A signal is obtained when [³H]-GDP complexes of Rho bind to RhoGAP. The affinity of the interaction was obtained by varying the concentration of Rho·[³H]GDP at a fixed concentration of GST-RhoGAP (Figure 1A). In the presence of 2 mM MgCl₂, 20 mM NaF, and 0.11 mM AlCl₃, a hyperbolic increase in the SPA signal was observed, giving an apparent K_d of 0.48 μ M. The experiment was repeated in the absence of added aluminum and presence of 1 mM deferoxamine, a powerful chelator of aluminum with a K_d of $\sim 10^{-20}$ M (28). Again, a hyperbolic increase in the SPA signal was observed, giving an apparent K_d of 0.28 μ M (Figure 1A).

The interaction between Ras·[³H]GDP and the GAP domain of NF1 was investigated using similar SPA binding experiments (Figure 1B). In the presence of 1 mM MgCl₂, 20 mM NaF, and 0.11 mM AlCl₃, Ras·[³H]GDP bound to GST-NF1 with an apparent K_d of 0.16 μ M. In the absence of added aluminum and in the presence of 1 mM deferoxamine, the binding of Ras·[³H]GDP to GST-NF1 was almost identical (apparent K_d of 0.13 μ M). Thus, Ras·GDP binding to NF1, like that of Rho·GDP to RhoGAP, can occur in the absence of added aluminum.

Sternweis and Gilman (12) originally described how contaminating aluminum was required for activation of heterotrimeric G proteins by fluoride. Thus, it was important to rigorously demonstrate that the binding between Rho·GDP and RhoGAP or between Ras·GDP and NF1 was not mediated by trace amounts of aluminum. The aluminum content of the buffers was found to be undetectable (<0.05 μ M), and the addition of deferoxamine made certain that any effects could not be attributed to free Al³⁺. To demonstrate that aluminum did not bind to the complex with extremely high affinity such that it was not removed by deferoxamine, we made use of ¹⁹F NMR and SPAs. ¹⁹F NMR spectra of a solution of AlCl₃ and NaF at pH 7.5 showed a resonance at -120 ppm, due to free fluoride ions, and resonances in the region of -155 ppm due to solvated aluminum fluoride species, AlF_x (Figure 2a) (29, 30). It should be noted that in similar NMR experiments at pH 8, these AlF_x NMR signals are not visible (10, 31). Addition of Rho·GDP did not perturb these signals (Figure 2b). However, subsequent addition of RhoGAP resulted in a reduction in the integral of these resonances and the appearance of a new resonance at -143 ppm (Figure 2c). When mutant RhoGAP, in which the catalytic Arg-282 has been mutated to Ala, replaced wild-type RhoGAP, this resonance was seen at -144.5 ppm (Figure 2d). Mixing R282A and wild-type RhoGAP (Figure 2e) resulted in a mixture of the two species in proportions consistent with their reported relative affinities (11), eliminating the possibility that chemical shift differences between the NMR

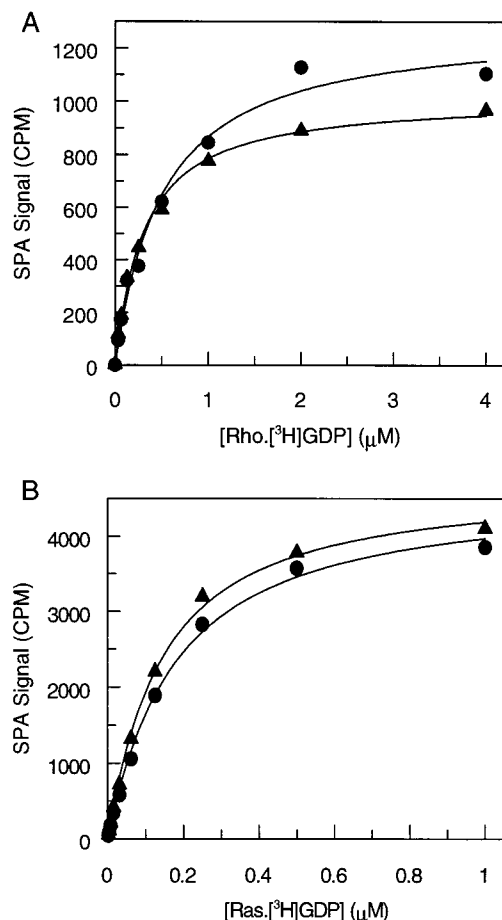


FIGURE 1: The aluminum chelator, deferoxamine, does not affect binding of Rho·GDP to RhoGAP (A) or Ras·GDP to NF1 (B) in the presence of NaF and MgCl₂. SPAs were performed in which the concentration of Rho·[³H]GDP was varied in the presence of 0.04 μM GST-RhoGAP (A) or the concentration of Ras·[³H]GDP was varied in the presence of 0.03 μM GST-NF1 (B). Experiments were performed in the presence of 0.11 mM AlCl₃ and absence of deferoxamine (●), or in the absence of AlCl₃ and presence of 1 mM deferoxamine (▲). Measurements on Rho were carried out in 20 mM Tris/HCl, pH 7.5, 2 mM MgCl₂, 20 mM NaF, and 1 mM DTT. Measurements on Ras were carried out in 50 mM Tris/HCl, pH 7.5, 1 mM MgCl₂, 20 mM NaF, and 2 mM DTT. The SPA signals from assays in which GST-RhoGAP or GST-NF1 were omitted were subtracted from those in their presence, and these values are plotted against the added concentration of radiolabeled Rho·GDP or Ras·GDP. The solid lines show the best fits to binding isotherms, with apparent K_{d} s of 0.48 and 0.28 μM for Rho/RhoGAP and 0.16 and 0.13 μM for Ras/NF1 in the absence and presence of deferoxamine, respectively.

signals were artifacts due to pH or other changes upon addition of proteins. These data are consistent with literature reports (10, 29, 31) that the signals between -143 and -145 ppm are from fluorine atoms in the Rho·GDP·AlF₃·RhoGAP complex. Deferoxamine completely removed the aluminum-dependent ¹⁹F NMR signal seen with wild-type RhoGAP (Figure 2f), demonstrating that it was able to extract aluminum from the preformed protein complex. Additionally, we found that deferoxamine prevented aluminum-dependent formation of complexes (at low Mg concentrations) in the SPA assay (data described below, shown in Figure 5).

Taken all together, these experiments prove that, under these conditions, aluminum is not required for fluoride-mediated binding of the GDP forms of either Rho or Ras to their GAPs.



FIGURE 2: ¹⁹F NMR spectra of Rho·GDP and RhoGAP in the presence of AlCl₃ and NaF. All ¹⁹F NMR spectra were recorded in buffer containing 50 mM Tris/HCl, pH 7.5, 5 mM NaF, 1 mM AlCl₃, 1 mM MgCl₂, and 5% D₂O. Spectra were recorded in the absence of protein (a), after addition of 200 μM Rho·GDP (b), and following subsequent addition of 200 μM wild-type RhoGAP (c). In a separate experiment, 200 μM Rho·GDP and 200 μM mutant R282A RhoGAP were mixed (d) followed by addition of 166 μM wild-type RhoGAP (e). After recording spectrum c in the presence of Rho·GDP and wild-type RhoGAP, 2.5 mM deferoxamine was added and the spectrum re-recorded (f). For spectra a–e 3000 scans and for spectrum f 1666 scans were acquired. The spectra are scaled accordingly.

Requirements for High-Affinity Binding of Rho·GDP to RhoGAP and Ras·GDP to NF1 in the Absence of Aluminum.

Next we examined the requirements for fluorine-mediated binding in the absence of aluminum (presence of 1 mM deferoxamine). Binding of either Rho·[³H]GDP to GST-RhoGAP (Figures 3A and 4A) or Ras·[³H]GDP to GST-NF1 (Figures 3B and 4B) was only detectable when both MgCl₂ and NaF were present. At 20 mM NaF, complex formation with both Rho and Ras showed a hyperbolic dependence upon the concentration of MgCl₂ with apparent K_{d} s of 1.1 and 1.2 mM, respectively (Figure 3). However, at fixed concentrations of MgCl₂, a sigmoidal dependence of Rho/RhoGAP or Ras/NF1 complex formation on the concentration of NaF was observed (Figure 4). These data were fitted to the Hill equation: $\text{SPA signal} = S_{\text{max}}[\text{NaF}]^n / (K^n + [\text{NaF}]^n)$, where S_{max} = maximum SPA signal, K = concentration for half-maximal binding, and n = Hill coefficient, giving Hill coefficients of 2.2 and 2.4 and concentrations for half-maximal binding of 19 and 20 mM for Rho and Ras, respectively. These data show that high-affinity complex formation of Rho·GDP or Ras·GDP with their GAPs, in the absence of aluminum, requires both fluoride and magnesium.

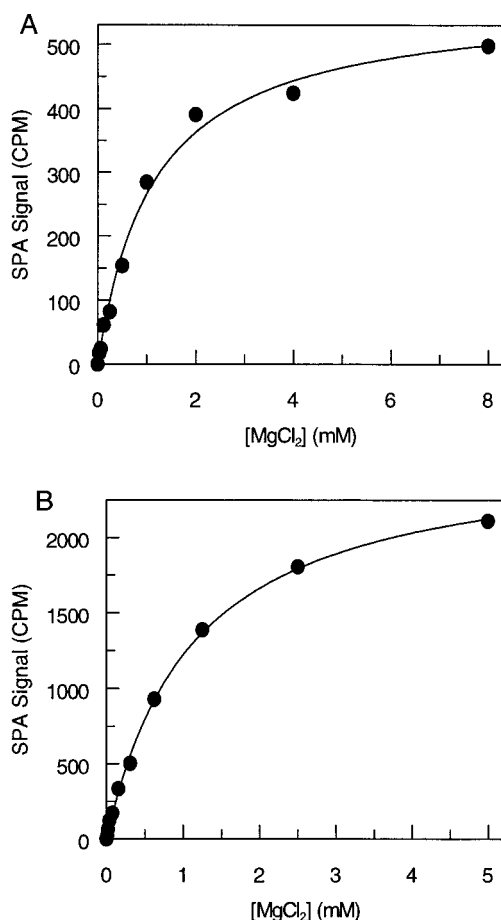


FIGURE 3: Effect of MgCl_2 concentration on binding of Rho-GDP to RhoGAP (A) or Ras-GDP to NF1 (B) in the presence of NaF and deferoxamine. SPAs were performed in which the concentration of MgCl_2 was varied in the presence of $0.04 \mu\text{M}$ GST-RhoGAP and $0.25 \mu\text{M}$ Rho- ^{3}H GDP (A) or $0.03 \mu\text{M}$ GST-NF1 and $0.2 \mu\text{M}$ Ras- ^{3}H GDP (B). Measurements on Rho were carried out in 2 mM MgCl_2 , 20 mM NaF, and 1 mM deferoxamine. Measurements on Ras were carried out in 1 mM MgCl_2 , 20 mM NaF, and 1 mM deferoxamine. The SPA signals from assays in which GST-RhoGAP or GST-NF1 were omitted were subtracted from those in their presence, and these values are plotted against the added concentration of MgCl_2 . The solid lines show the best fits to binding isotherms with apparent K_d s of 1.1 mM for Rho/RhoGAP and 1.2 mM for Ras/NF1.

An attempt was made to observe the formation of an aluminum-independent, magnesium-dependent, fluoride-containing Rho-GDP-RhoGAP complex by ^{19}F NMR. In line with literature observations (31), addition of 1 mM MgCl_2 to a 5 mM solution of NaF results in the broadening of the free F^- signal at -120 ppm within the ^{19}F NMR spectrum, neither altering the chemical shift of the peak nor producing additional signals. This is consistent with the formation of MgF_x on an intermediate NMR exchange time scale. Under conditions where the formation of a magnesium-dependent Rho-GDP-RhoGAP complex would be expected, no new ^{19}F resonances were observed. The absence of new resonances is likely to be due to the exchange rate between the free and complex ions being rapid compared to the chemical shift difference.

Requirements for High-Affinity Binding of Rho-GDP to RhoGAP and Ras-GDP to NF1 in the Presence of Aluminum and $10 \mu\text{M}$ MgCl_2 . Since we have shown that magnesium is required for fluoride-dependent high-affinity complex forma-

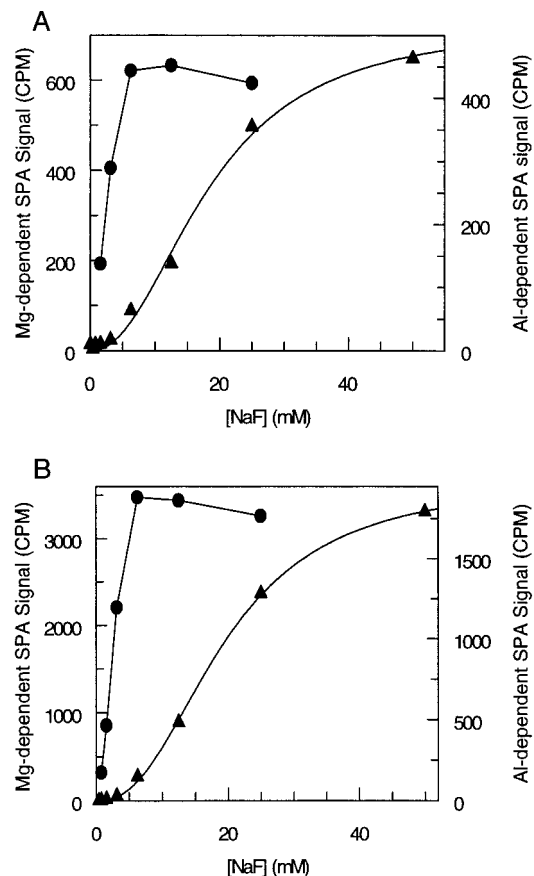


FIGURE 4: Effect of NaF concentration on binding of Rho-GDP to RhoGAP (A) or Ras-GDP to NF1 (B) in the presence of either MgCl_2 plus deferoxamine or AlCl_3 . SPAs were performed as in Figure 3 except that the concentration of NaF was varied with either 2 mM (Rho/RhoGAP) or 1 mM (Ras/NF1) MgCl_2 (\blacktriangle). The solid lines are the best fits to the Hill equation, giving Hill coefficients of 2.2 and 2.4 and concentrations for half-maximal binding of 19 and 20 mM for Rho/RhoGAP and Ras/NF1, respectively. SPAs were also performed with $10 \mu\text{M}$ MgCl_2 and AlCl_3 (\bullet). Data below 1.5 mM NaF are not plotted as the blanks were high compared to the signal.

tion in the absence of aluminum (Figure 3), and addition of aluminum at high magnesium concentration did not greatly affect complex formation (Figure 1), we addressed whether aluminum could promote complex formation at low magnesium concentrations. Small G proteins are unstable in the absence of magnesium. Therefore, we performed experiments at $10 \mu\text{M}$ MgCl_2 , a concentration which is sufficiently low for no significant complex formation to occur (Figure 3), but high enough to give a stable SPA signal for several hours. In the presence of 20 mM NaF, there was a hyperbolic dependence of high-affinity Rho-GDP/RhoGAP complex formation on AlCl_3 concentration (Figure 5A), showing that aluminum can promote complex formation at low concentrations of magnesium. The apparent K_d for aluminum was calculated to be 0.19 mM . As expected, inclusion of excess deferoxamine prevented complex formation. Likewise, there was a hyperbolic dependence of high-affinity Ras-GDP/NF1 complex formation upon AlCl_3 concentration, with an apparent K_d of 0.23 mM (Figure 5B). Again, inclusion of excess deferoxamine prevented complex formation. Thus, aluminum can promote complex formation of both Rho-GDP with RhoGAP and Ras-GDP with NF1 at low concentrations of magnesium.

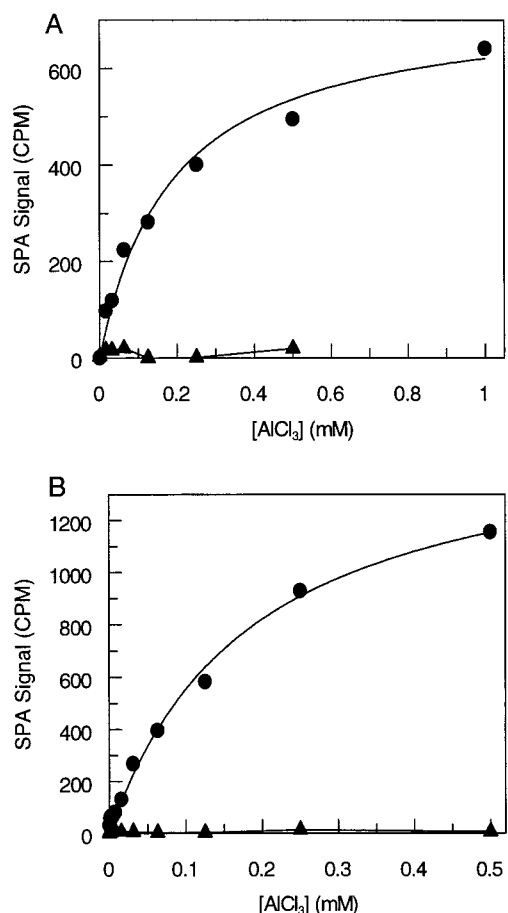


FIGURE 5: Effect of $AlCl_3$ concentration on binding of Rho•GDP to RhoGAP (A) or Ras•GDP to NF1 (B) in the presence of 10 μ M $MgCl_2$ and NaF. SPAs were performed as in Figure 3 except that the concentration of $AlCl_3$ was varied in the presence of 10 μ M $MgCl_2$. Experiments were performed in the absence (●) or presence of 1 mM deferoxamine (▲). The solid lines shown for data in the absence of deferoxamine are the best fits to binding isotherms, with apparent K_d s of 0.19 and 0.23 mM for Rho/RhoGAP and Ras/NF1, respectively.

To address the dependence of AlF_x -mediated complex formation on NaF concentration, we varied the NaF concentration at 10 μ M $MgCl_2$ (Figure 4). However, as the concentration of NaF was reduced below 1 mM, the control SPA signal in the absence of GST–GAP became markedly increased, such that the interpretation of assays was unclear. Very likely this was caused by insolubility of aluminum hydroxide. At concentrations of NaF above 20 mM, there was a decline in the GAP-dependent signal. Despite these limitations, the curves were distinctly sigmoidal rather than hyperbolic (Figure 4). We could estimate the concentration of NaF required for the half-maximal effect as about 2.5 mM, with saturation at less than 6 mM, both for Rho and for Ras.

Binding affinities in the presence of aluminum were determined in similar experiments to those in Figure 1 but with 10 μ M $MgCl_2$ (data not shown). The dose–responses were hyperbolic, and the apparent K_d s for Rho•GDP and RhoGAP or Ras•GDP and NF1 at 6 mM NaF were 0.17 and 0.52 μ M, respectively. Experiments with Ras at 20 mM NaF showed that the affinity was almost unchanged, consistent with saturation at 6 mM.

Fluoride-Mediated Interaction between Rho•GDP and Mutant R282A RhoGAP. Experiments similar to those in

Figure 1 were used to determine binding affinities of GST–R282A RhoGAP and Rho•GDP. The apparent K_d in the presence of 0.11 mM $AlCl_3$ and 2 mM $MgCl_2$ was 1.4 μ M, in the presence of 2 mM $MgCl_2$ and 1 mM deferoxamine was 4.9 μ M, and in the presence of 0.11 mM $AlCl_3$ and 10 μ M $MgCl_2$ was 0.9 μ M.

DISCUSSION

As previously reported, AlF_x mediates high-affinity binding of Rho•GDP to RhoGAP (Figures 1A and 5A and references 6, 10, 11, 32) and of Ras•GDP to NF1 (Figures 1B and 5B and references 3, 4, 32). However, we also found a similar degree of binding of either Rho•GDP or Ras•GDP to their respective GAPs even when no aluminum was added (Figures 1A and B). Fluoride-dependent activation of heterotrimeric G proteins was previously attributed to contamination by aluminum (12). The following evidence suggested that the binding observed here was not due to contaminating aluminum: (i) Direct measurement of the aluminum concentration in the buffers showed that it was $<0.05 \mu$ M. (ii) Addition of 1 mM deferoxamine, which chelates aluminum with extremely high affinity (28), did not block fluoride-mediated complex formation at high magnesium concentrations (Figure 1). (iii) Deferoxamine can chelate aluminum from the small G protein/GAP/ AlF_x complex (Figures 2 and 5).

The data shown in Figures 3 and 4 demonstrate that fluoride-mediated, aluminum-independent complex formation of Rho•GDP and Ras•GDP with their respective GAPs requires the presence of fluoride and high concentrations of magnesium. These data support the conclusion of Vincent et al. (24) that fluoride-mediated Rho•GDP binding to p190 RhoGAP (GAP domain homologous to that in RhoGAP described here) did not absolutely require aluminum but was supported by magnesium. Importantly, we show that this phenomenon is more general to small G proteins as almost identical results were obtained here with Ras•GDP and NF1. As heterotrimeric G proteins can also be activated by fluoride in a magnesium-dependent, aluminum-independent manner (21–23), magnesium fluoride activation of other GTP binding proteins, and indeed other nucleotide binding proteins, may well be possible.

The use of equilibrium binding assays has allowed us to quantify, for the first time, the requirements for fluoride-mediated binding of the GDP forms of Rho and Ras to their GAPs. Although these systems with many reactants and complex solution chemistry (30, 33) prevent a complete analysis, many significant conclusions can be made. The requirements for both magnesium- and aluminum-dependent fluoride-mediated binding were remarkably similar for Rho and Ras. Thus, at 20 mM NaF, $MgCl_2$ promoted binding of Rho (Figure 3A) and Ras (Figure 3B) with apparent K_d values of 1.1 and 1.2 mM, respectively. At the same concentration of NaF, in the presence of 10 μ M $MgCl_2$, $AlCl_3$ promoted binding of Rho (Figure 5A) and Ras (Figure 5B) with apparent K_d values of 0.19 and 0.23 mM, respectively. The concentrations of fluoride required for the half-maximal effect were much higher for magnesium-dependent (20 mM) than for aluminum-dependent (2.5 mM) binding (Figure 4). Again, the requirements were similar for Rho (Figure 4A) and for Ras (Figure 4B). In the absence of aluminum, the

apparent affinities of Rho•GDP and of Ras•GDP for their GAPs, in the presence of approximately half-saturating concentrations of NaF and of MgCl_2 , were found to be 0.28 μM (Rho; Figure 1A) and 0.13 μM (Ras; Figure 1B). With 10 μM MgCl_2 and 0.11 mM AlCl_3 , the affinity of Rho for its GAP was slightly higher (K_d 0.17 μM), whereas that of Ras for its GAP was slightly weaker (K_d 0.52 μM). In conclusion, high concentrations of magnesium and of fluoride are required to obtain fluoride-mediated response in the absence of aluminum. In contrast, the aluminum-mediated response requires lower concentrations of both aluminum and fluoride. It should be noted, however, at approximately half-saturating concentrations of magnesium fluoride or of aluminum fluoride, the affinities of Rho•GDP or of Ras•GDP for their GAPs are all close to each other (apparent K_d ca. 0.1–0.5 μM). Thus, either aluminum or magnesium is able to effectively mediate complex formation in the presence of fluoride.

The results seen here with Ras and Rho are qualitatively similar to those seen with G_α . With each protein, aluminum allows activation with much lower concentrations of fluoride than that required to obtain magnesium-dependent effects, and for the latter millimolar concentrations of MgCl_2 are required (Figures 3 and 4 and references 21–23). However, there are quantitative differences in that the concentrations of aluminum required for half-maximal activation of G_α are 1–5 μM (15), about 2 orders of magnitude less than for Rho or Ras.

In the absence of aluminum, fluoride-dependent complex formation of both Ras and Rho with their respective GAPs showed simple, hyperbolic dependences upon the concentration of magnesium (Figure 3). However, with both complexes, the dependence upon the concentration of fluoride was sigmoidal (Figure 4). The data were fitted to the Hill equation with Hill coefficients of 2.2 and 2.4. These values are empirical fits but are consistent with several fluoride molecules being required as part of the stable complex. The mechanistic implications of Hill coefficients greater than unity are discussed in detail in reference 34, where it is concluded that the Hill coefficient provides only a lower limit on the real stoichiometry. Such behavior was not previously studied with Rho (24), but is similar to that reported for fluoride-dependent activation of transducin (22). In the latter case, the Hill coefficients obtained, taken in conjunction with kinetic measurements (23), were interpreted as supporting a model in which there is formation of a $\text{GDP}\cdot\text{MgF}_3$ complex, mimicking the γ -phosphate of GTP.

X-ray diffraction structures of $\text{Cdc42}\cdot\text{Cdc42GAP}$ (20) and of $\text{Rho}\cdot\text{RhoGAP}$ (6) complexes crystallized in the presence of aluminum fluoride have been reported. Cdc42 and Rho are highly homologous proteins, and the domains of Cdc42GAP and RhoGAP used for these studies were identical. Thus, one might have anticipated that the structures around the conserved active site would be near-identical. However, the Cdc42 -containing structure contained a central metal ion coordinated to three equatorial fluorine atoms, an axial oxygen atom from the β -phosphate of the nucleoside diphosphate, and an axial water molecule; this was interpreted as AlF_3 . In contrast, in the Rho-containing structure, the metal ion is octahedrally coordinated with four equatorial fluoride ions, and this was interpreted as AlF_4^- . We note that for the crystallization of the $\text{Cdc42}\cdot\text{GDP}\cdot\text{AlF}_3\cdot\text{Cdc42GAP}$

complex high concentrations of magnesium (100 mM) and low aluminum concentrations (0.08 mM) were used (20). Under these conditions, it is likely, from the data presented here, that the complexes formed do not contain AlF_3 as originally assumed, but in fact contain MgF_3^- . This is supported by the X-ray diffraction structure of the complex of $\text{Rho}\cdot\text{GDP}$ and RhoGAP in the presence of fluoride and magnesium, but absence of aluminum (J. F. Eccleston, S. J. Gamblin, D. L. Graham, K. Rittinger, and S. J. Smerdon, unpublished observations). This shows a central metal ion with a trigonal bipyramidal arrangement of ligands around it; this is the same configuration as observed in the proposed $\text{Cdc42}\cdot\text{GDP}\cdot\text{AlF}_3\cdot\text{Cdc42GAP}$ complex.

NDP kinase (18), UMP kinase (19), and $\text{Ras}\cdot\text{RasGAP}$ (4) have been crystallized in the presence of aluminum fluoride and reported to contain an AlF_3 species. As discussed by Schlichting and Reinstein (19), AlF_3 is not the most abundant aluminum fluoride species under the crystallization conditions used, but it was proposed that the enzyme precisely fits only the AlF_3 species. However, we note that high millimolar concentrations of magnesium were present in all cases, and hence it seems quite plausible that some (or even all) of these structures might in fact contain a MgF_3^- species. We found that the concentration of fluoride required for maximal aluminum-mediated binding is very much lower than that for magnesium-mediated binding. Hence, higher fluoride concentrations will increase the likelihood of magnesium fluoride rather than AlF_x binding, though the species bound will also reflect its affinity for the protein. Furthermore, it is likely that the structure of magnesium fluoride activated G_α (21–23), which has not yet been determined, would show a trigonal pyramidal arrangement rather than the previously proposed tetrahedral arrangement (22). It is noteworthy that such MgF_3^- complexes would be expected to mimic the transition state of hydrolysis very closely both in charge and in geometry.

We recently suggested that the AlF_x -mediated complex between $\text{Rho}\cdot\text{GDP}$ and RhoGAP did not have all the thermodynamic properties expected of the transition state though it might well be a close structural analogue (11). This was based on two observations. First, RhoGAP bound to $\text{Rho}\cdot\text{GDP}$, in the presence of AlF_x , with similar affinity as to $\text{Rho}\cdot\text{GTP}$. Second, removal of the catalytic arginine residue of RhoGAP reduced catalysis by 230-fold, but AlF_x -mediated binding of the mutant RhoGAP to $\text{Rho}\cdot\text{GDP}$ was only reduced 2–4-fold. The apparent affinity of the magnesium fluoride-mediated complex is not very significantly different from the AlF_x -mediated complex, suggesting that it is not a dramatically closer thermodynamic mimic of the transition state. We also looked at the properties of the R282A RhoGAP mutant. The NMR experiments shown in Figure 2 confirmed that R282A RhoGAP binds to $\text{Rho}\cdot\text{GDP}$ in the presence of AlF_x . Interestingly, the resonance from the bound AlF_x species was shifted upfield relative to that of wild-type RhoGAP . This upfield shift is consistent with the removal of the arginine from the fluorine coordination sphere and the X-ray structure of $\text{Cdc42}\cdot\text{GDP}$ bound to R305A (equivalent to R282A) Cdc42GAP , which shows an altered arrangement of residues around the AlF_x species (20). We found that the R282A mutation caused a 17-fold decrease in binding affinity for MgF_x -mediated complex formation but only 5-fold for AlF_x -mediated complex formation,

suggesting that the MgF_3 species might be a slightly closer approximation to the transition state. However, irrespective of whether mediated by MgF_x or by AlF_x , the R282A mutant does not show the loss of affinity to Rho•GDP that might be anticipated from the catalytic enhancement provided by Arg-282 if these fluoride complexes are close thermodynamic transition state analogues (11).

In conclusion, it has now been demonstrated that both heterotrimeric G proteins and small G proteins can form aluminum-independent, magnesium-dependent complexes with fluoride, suggesting this might be a more general property of nucleotide binding proteins. Furthermore, it is possible that some X-ray structures previously interpreted as containing aluminum fluoride might in fact contain magnesium fluoride.

ACKNOWLEDGMENT

We are very grateful to S. J. Gamblin, K. Rittinger, and S. J. Smerdon for suggestions and discussions. We thank A. Hall for expression plasmids for RhoGAP and Rho, S. Graham for mass spectrometry analysis, M. Goggin for large-scale fermentation, and S. Francis for aluminum analysis in buffers.

REFERENCES

1. Mackay, D. J. G., and Hall, A. (1999) *J. Biol. Chem.* 273, 20685–20688.
2. Vojtek, A. B., and Der, C. J. (1999) *J. Biol. Chem.* 273, 19925–19928.
3. Mittal, R., Ahmadian, M. R., Goody, R. S., and Wittinghofer, A. (1996) *Science* 273, 115–117.
4. Scheffzek, K., Ahmadian, M. R., Kabsch, W., Wiesmuller, L., Lautwein, A., Schmitz, F., and Wittinghofer, A. (1997) *Science* 277, 333–338.
5. Ahmadian, M. R., Stege, P., Scheffzek, K., and Wittinghofer, A. (1997) *Nat. Struct. Biol.* 4, 686–689.
6. Rittinger, K., Walker, P. A., Eccleston, J. F., Smerdon, S. J., and Gamblin, S. J. (1997) *Nature* 389, 758–762.
7. Li, R., Zhang, B., and Zheng, Y. (1997) *J. Biol. Chem.* 272, 32830–32835.
8. Sermon, B. A., Lowe, P. N., Strom, M., and Eccleston, J. F. (1998) *J. Biol. Chem.* 273, 9480–9485.
9. Leonard, D. A., Lin, R., Cerione, R. A., and Manor, D. (1998) *J. Biol. Chem.* 273, 16210–16215.
10. Hoffman, G. R., Nassar, N., Oswald, R. E., and Cerione, R. A. (1998) *J. Biol. Chem.* 273, 4392–4399.
11. Graham, D. L., Eccleston, J. F., and Lowe, P. N. (1999) *Biochemistry* 38, 985–991.
12. Sternweis, P. C., and Gilman, A. G. (1982) *Proc. Natl. Acad. Sci. U.S.A.* 79, 4888–4891.
13. Bigay, J., Deterre, P., Pfister, C., and Chabre, M. (1985) *FEBS Lett.* 191, 181–185.
14. Bigay, J., Deterre, P., Pfister, C., and Chabre, M. (1987) *EMBO J.* 6, 2907–2913.
15. Sondek, J., Lambright, D. G., Noel, J. P., Hamm, H. E., and Sigler, P. B. (1994) *Nature* 372, 276–279.
16. Coleman, D. E., Berghuis, A. M., Lee, E., Linder, M. E., Gilman, A. G., and Sprang, S. R. (1994) *Science* 265, 1405–1412.
17. Fisher, A. J., Smith, C. A., Thoden, J. B., Smith, R., and Sutoh, K. (1995) *Biochemistry* 34, 8960–8972.
18. Xu, Y. W., Morera, S., Janin, J., and Cherfils, J. (1997) *Proc. Natl. Acad. Sci. U.S.A.* 94, 3579–3583.
19. Schlichting, I., and Reinstein, J. (1997) *Biochemistry* 36, 9290–9296.
20. Nassar, N., Hoffman, G. R., Manor, D., Clardy, J. C., and Cerione, R. A. (1998) *Nat. Struct. Biol.* 5, 1047–1052.
21. Higashijima, T., Ferguson, K. M., Sternweis, P. C., Ross, E. M., Smigel, M. D., and Gilman, A. G. (1987) *J. Biol. Chem.* 262, 752–756.
22. Antonny, B., Bigay, J., and Chabre, M. (1990) *FEBS Lett.* 268, 277–280.
23. Antonny, B., Sukumar, M., Bigay, J., Chabre, M., and Higashijima, T. (1993) *J. Biol. Chem.* 268, 2393–2402.
24. Vincent, S., Brouns, M., Hart, M. J., and Settleman, J. (1998) *Proc. Natl. Acad. Sci. U.S.A.* 95, 2210–2215.
25. Eccleston, J. F., Moore, K. J., Morgan, L., Skinner, R. H., and Lowe, P. N. (1993) *J. Biol. Chem.* 268, 27012–27019.
26. Penefsky, H. S. (1977) *J. Biol. Chem.* 252, 2891–2899.
27. Gorman, C., Skinner, R. H., Skelly, J. V., Neidle, S., and Lowe, P. N. (1996) *J. Biol. Chem.* 271, 6713–6719.
28. Evers, A., Hancock, R. D., Martell, A. E., and Motekaitis, R. J. (1989) *Inorg. Chem.* 28, 2189–2195.
29. Maruta, S., Henry, G. D., Sykes, B. D., and Ikebe, M. (1993) *J. Biol. Chem.* 268, 7093–7100.
30. Martinez, E. J., Girardet, J. L., and Morat, C. (1996) *Inorg. Chem.* 35, 706–710.
31. Higashijima, T., Graziano, M. P., Suga, H., Kainosho, M., and Gilman, A. G. (1991) *J. Biol. Chem.* 266, 3396–3401.
32. Ahmadian, M. R., Mittal, R., Hall, A., and Wittinghofer, A. (1997) *FEBS Lett.* 408, 315–318.
33. Martin, R. B. (1996) *Coord. Chem. Rev.* 149, 23–32.
34. Wells, J. W. (1992) in *Receptor–Ligand Interactions; A Practical Approach* (Hulme, E. C., Ed.) pp 289–395, IRL Press, Oxford, U.K.

BI991358E